Role of A_1 receptor-activated GIRK channels in the suppression of hippocampal seizure activity

Emily Hill, Charlotte Hickman, Rebecca Diez and Mark Wall*

School of Life Sciences

University of Warwick

Gibbet Hill

Coventry

CV4 7AL

Author correspondence

Mark Wall

School of Life Sciences

University of Warwick

Gibbet Hill

Coventry

CV4 7AL

Mark.wall@warwick.ac.uk

Abstract

The neuromodulator adenosine is released during seizure activity to provide negative feedback suppression of on-going activity and to delay the occurrence of the next burst of activity. Adenosine acts via multiple G protein coupled receptors including the A_1 receptor (A_1R) which inhibits neurotransmitter release and hyperpolarises neuronal membrane potential. The hyperpolarisation is produced, at least in part, by the activation of G protein-activated inwardly rectifying K^+ (GIRK) channels. We have used tertiapin-Q (TQ), a potent and selective inhibitor of GIRK channels, to assess the role of GIRK channels in controlling seizure activity in areas CA1 and CA2 of mouse hippocampal slices. TQ (100-300 nM) blocked ~50 % of the adenosine-mediated membrane potential hyperpolarisation of hippocampal CA1 and CA2 neurons. TQ (100 nM) had no significant effect on synaptic transmission in area CA1 of the hippocampus but enhanced transmission in CA2, an effect prevented by blocking A_1Rs. TQ (100 nM) increased the frequency of spontaneous activity (induced by removing Mg^{2+} and increasing K^+) and blunted the effects of exogenous adenosine on the suppression of activity. TQ had a significantly greater effect on electrically-stimulated seizure activity induced in CA2 versus that in CA1, producing a greater increase in both the duration and amplitude of the stimulated bursts. This is consistent with the greater A_1R density and A_1R activation tone in CA2. Thus GIRK channels play a role in the supressing effects of adenosine on seizure activity.

1. Introduction

The activity-dependent release of the neuromodulator adenosine into the extracellular space leading to the activation of A_1 receptors (A_1Rs) and suppression of network activity is a common mechanism for preventing neural network over-excitation across the brain (During and Spencer, 1992, reviewed in Boison, 2013, Frenguelli and Wall, 2015). Adenosine is released into the extracellular space either as ATP, which is subsequently metabolised to adenosine (Newman et al., 2004; Pankratov et al., 2007) or is directly released via equilibrative nucleoside transporters (ENTs, Wall and Dale, 2013; Diez et al., 2017) or by exocytosis (Klyuch et al., 2012). The subsequent modulation of neural activity via A_1R activation has a wide dynamic range, supressing activity that ranges from low-rate population spike-like activity to high-rate pathological epileptiform bursts (Wall and Richardson, 2015). The activation of A_1Rs supresses activity through two major mechanisms: the presynaptic inhibition of synaptic transmission and by the hyperpolarisation of neuronal membrane potential (Dunwiddie and Fredholm, 1989; Thompson et al., 1992; Kerr et al., 2013). The precise importance of these two processes in the inhibitory control of neural activity by A_1R activation remains unclear and will probably depend on the type of activity and brain area.

Adenosine hyperpolarises neuronal membrane potential through the activation of specific K^+ channels (Trussell and Jackson, 1985; 1987). These K^+ channels include G protein-activated inwardly rectifying K^+ (GIRK) channels (K_{IR}3.1-4; Sickmann and Alzheimer, 2003; Clark et al., 2009; Kim and Johnston, 2015). GIRK channels have a wide distribution across the brain and are not only opened by A_1Rs but also by a wide-variety of ligand gated G protein receptors including $GABA_{B,}$ muscarinic, adrenergic and dopaminergic receptors (reviewed in Kobayashi and Ikeda, 2006). GIRK channels are selectively blocked by tertiapin, which is a 21 amino acid peptide from the venom of the European honey bee (Gauldie et al., 1976). Tertiapin-Q (TQ) is a stable tertiapin derivative which retains the potency but does not undergo oxidation (Jin and Lu, 1999). TQ has a reported IC_{50} for GIRK channels of 10 nM

(Jin and Lu, 1998) but is often used in brain slices at a concentration between 30-300 nM (Breton and Stuart, 2017; Takigawa and Alzheimer, 2002; Kim and Johnson, 2015). It has also been reported that TQ can block large conductance Ca^{2+} activated potassium channels (BK) with a similar potency to GIRK channels (IC_{50} ~ 5-10 nM, Kanjhan et al ., 2005). However the block of BK channels has slow kinetics taking ~ 15 minutes to reach steady state whereas GIRK channels are completely blocked within 1-2 minutes of TQ application (Kanjhan et al., 2005).

In this study we have used short duration applications of TQ (10-15 minutes) to investigate the importance of GIRK channel activation in the A_1R-mediated control of seizure-like activity in the hippocampus from young mice (P12-18) and from adult mice (2-3 months). We have chosen to do experiments in two ages of mice because of the reported differences in adenosine receptor tone (for example see Kerr et al 2013 but see Dumas and Foster 1998). There is strong expression of A_1Rs across the hippocampus but the expression is particularly enriched in area CA2 (Ochiishi et al., 1999). It has also been shown that block of A_1Rs in CA2, with caffeine, leads to the robust potentiation of synaptic transmission that does not occur in other regions of the hippocampus (Simons et al., 2011). Our data suggests that the greater activation of GIRK channels in CA2 preferentially supresses seizure activity in CA2 vs CA1.

2. Methods

2.1 Preparation of hippocampal slices

All animal care and experimental procedures were reviewed and approved by the institutional animal welfare and ethical review body (AWERB) at the University of Warwick.

Parasagittal slices of hippocampus (400 μm) were prepared from male C57BL/6 mice, at postnatal days 12-65 (Wall et al., 2018). Mice were kept on a 12-hour light-dark cycle with slices made 90 minutes after entering the light cycle. In accordance with the U.K. Animals

(Scientific Procedures) Act (1986), mice were killed by cervical dislocation and then decapitated. The brain was removed, cut down the mid-line and the two sides of the brain stuck down to the base plate. Slices were cut around the midline with a Microm HM 650V microslicer in cold (2-4°C) high Mg^{2+}, low Ca^{2+} aCSF, composed of (mM): 127 NaCl, 1.9 KCl, 8 $MgCl_2$, 0.5 $CaCl_2$, 1.2 KH_2PO_4, 26 $NaHCO_3$, 10 D-glucose (pH 7.4 when bubbled with 95% O_2 and 5% CO_2, 300 mOSM). Slices were stored at 34°C for 1-6 hours in aCSF (1 mM $MgCl_2$, 2 mM $CaCl_2$) before use.

2.2 Extracellular recording of synaptic transmission from hippocampal slices

A slice was transferred to the recording chamber, submerged in aCSF and perfused at 4-6 ml/min (32°C). The slice was placed on a grid allowing perfusion above and below the tissue and all tubing (Tygon) was gas tight (to prevent loss of oxygen). For extracellular recording, an aCSF filled microelectrode was placed on the surface of stratum radiatum either in CA1 or in CA2. To evoke fEPSPs in CA1, the stimulating electrode was placed in CA3. To evoke fEPSPs in CA2, Schaffer collaterals (SC) were stimulated in CA1 (Chevaleyre and Siegelbaum, 2010; Simons et al., 2011; Munoz and Solis, 2018) Extracellular recordings were made using a differential model 3000 amplifier (AM systems, WA USA) with field EPSPs (fEPSPs) evoked with an isolated pulse stimulator model 2100 (AM Systems, WA). A 10-20 minute baseline was recorded at a stimulus intensity that gave 40-50 % of the maximal response. Signals were filtered at 3 kHz and digitised on line (10 kHz) with a Micro CED (Mark 2) interface controlled by Spike software (Vs 6.1, Cambridge Electronic Design, Cambridge UK). For fEPSP slope, a 1 ms linear region following the fibre volley was measured.

2.3 Whole cell patch clamp recording

A slice was transferred to the recording chamber and perfused at 3 ml min^{-1} with aCSF at 32 ± 0.5°C. Slices were visualized using IR-DIC optics with an Olympus BX51WI microscope (Scientifica) and a CCD camera (Hitachi). Whole-cell current clamp recordings were made from pyramidal cells area in the hippocampus using patch pipettes (5–10 MΩ) manufactured from thick walled glass (Harvard Apparatus, Edenbridge UK) and containing (mM): potassium gluconate 135, NaCl 7, HEPES 10, EGTA 0.5, phosphocreatine 10, MgATP 2, NaGTP 0.3 (290 mOSM, pH 7.2). Recordings were made from pyramidal cells in CA1 and also in CA2. Pyramidal cells were identified by their position in the slice and their current-voltage relationship (Chevaleyre and Siegelbaum 2010). CA2 neurons had a lower input resistance than CA1 neurons and CA2 neurons unlike CA3 neurons did not fire a burst of action potentials at the beginning of a depolarizing current step, instead fired during the entire depolarization (Fig 1A). CA2 neurons could further be distinguished from CA1 neurons because the prominent slow after-hyperpolarization present in CA1 neurons was absent in CA2 neurons. Finally, the depolarizing sag in response to a hyperpolarizing current pulse, which is caused by the hyperpolarization-activated cation current (Ih), was much larger in CA1 neurons than in CA2 neurons (Fig 1A; Chevaleyre and Siegelbaum 2010). We cannot be completely certain that all of the cells recorded from the CA2 region are all CA2 pyramidal cells because the neurons have not been reconstructed. Voltage and current recordings were obtained using an Axon Multiclamp 700B amplifier (Molecular Devices, USA) and digitised at 20 KHz. Data acquisition and analysis was performed using pClamp 10 (Molecular Devices, USA). All patch clamp recordings were made from slices from young mice (P12-18).

2.4 Seizure models

Two different solutions were used to induce seizure activity in hippocampal slices: 1) aCSF which contained no Mg^{2+} and with the total K^+ concentration increased from 3.1 to 6 mM (with

KCl) and 2) aCSF which contained no Mg^{2+} with a standard K^+ concentration (3.1 mM) Removal of extracellular Mg^{2+} facilitates NMDA receptor activation producing long lasting EPSPs which can sum together to produce tonic activation. Increasing the extracellular concentration of K^+ depolarises neurons leading to action potential firing and the release of glutamate to sustain activity. Both the increase in K^+ concentration and removal of Mg^{2+} are required to produce reliable spontaneous activity in 400 μm hippocampal slices (reviewed in Frenguelli and Wall 2016). The removal of Mg^{2+} leads to only sparse spontaneous activity but stimulation with a train of stimuli (60 Hz for 2s, Etherington and Frenguelli, 2004; Frenguelli and Wall, 2016) can reliably induce bursts of activity. To quantify these electrically-stimulated bursts, the number of spikes was measured following the end of the stimulation period and peak seizure amplitude was measured after the bursts had been rectified.

To investigate the spread of activity between the hippocampus and neocortex we used parasagittal slices taken close to the mid-line which were not trimmed (see Fig 6A). Recording electrodes were placed in stratum radiatum in area CA1 of the hippocampus and in layer 5 of the hind limb somatosensory cortex. To assess whether the neocortex was connected to the hippocampus we induced spontaneous activity with zero Mg^{2+}, 6 mM K^+ aCSF. If the two areas were connected then the activity was temporally coupled whereas if activity occurred independently then we assumed that the connections were absent or weak. The temporal correlation was assessed using the waveform correlation function in Spike (Vs 6.1, Cambridge Electronic Design, Cambridge UK). To stimulate activity, a stimulating electrode was placed in stratum radiatum of CA3 in slices in which there was some connection between the hippocampus and neocortex.

2.5 Drugs

Drugs were made up as stock solutions (1-10 mM) in distilled water and then diluted in aCSF. Adenosine, 8-cyclopentyltheophylline (8CPT) were obtained from Sigma (Dorset, UK). Tertiapin-Q and CGP35348 were obtained from (Tocris, Abingdon, UK).

2.6 Statistics

All quoted data is mean ± SEM. For statistical analysis paired t-test, unpaired students t-tests, one-way and two way ANOVA tests were performed.

3. Results

3.1 Tertiapin Q significantly reduces adenosine mediated hyperpolarisation of pyramidal cell membrane potential

To investigate the role that GIRK channels play in the membrane potential hyperpolarisation of hippocampal CA1 and CA2 neurons (Fig. 1A) produced by activating A_1Rs, we used the GIRK channel inhibitor tertiapin-Q (TQ,100-300 nM, Jin and Lu, 1999; Zhang et al., 2017). In interleaved slices, adenosine (100 μM) was either applied in control conditions or was applied to slices which had been pre-incubated in TQ for 10 minutes, with the TQ still present. The addition of TQ had no significant effect on the resting potential of either CA1 neurons (-65.8 ± 1.4 vs -65.7 ±1.4 mV, *n* = 9 slices Fig. 1B) or CA2 neurons (-66.7 ± 2.2 mV vs -66.5 ± 2.3 mV Fig 1B) and also did not change the holding current measured in voltage clamp (CA1 neurons held at -60 mV, *n* = 4). This suggests that there is very little basal activation of GIRK channels in either CA1 or CA2 pyramidal cells under quiescent conditions. In control, adenosine produced a mean membrane hyperpolarisation of 7.6 ± 0.7 mV of CA1 neurons (*n* = 6 slices, Fig. 1C, D) and a mean membrane hyperpolarisation of CA2 neurons of 7.8 ± 0.2 mV (*n* = 4 slices). In the presence of TQ (100 nM) this was significantly reduced (~50 %) to 3.77 ± 0.3 mV in CA1 neurons (*n* = 6 slices, Fig. 1C, D) and to 3.7 ± 0.4 mV in CA2 neurons. Increasing the concentration of TQ to 300 nM (*n* = 3) did not further reduce the hyperpolarisation produced by adenosine (3.65 ± 0.5 mV, Fig. 1D) in

CA1. Thus around 50 % of the hyperpolarisation produced by adenosine in both CA1 and CA2 pyramidal cells is via the activation of GIRK channels.

3.2 Tertiapin-Q has little effect on basal synaptic transmission in CA1 but enhances transmission in CA2

We next investigated the role that GIRK channels play in controlling basal synaptic transmission. Application of TQ (100 nM) had no significant effect on the slope of fEPSPs (0.9 ± 1.6 % increase, *n* = 14) or the paired pulse ratio of fEPSPs (at an interval of 50 ms, 1.75 ± 0.1 vs 1.76 ± 0.09 *n* = 5) that were evoked in CA1 (Fig. 2A, B). The A_1R antagonist 8-CPT (2 μM) also had little effect on the magnitude of fEPSP slope (8.4 ± 1 % increase, *n* = 5, Figure 2A, B). Therefore in CA1, there is little endogenous activation of A_1Rs under basal conditions and therefore little endogenous GIRK channel activity. The effects of TQ were also measured on the inhibitory effects of exogenous adenosine on synaptic transmission to CA1 neurons. Application of 20 μM adenosine (a concentration which is the approximate IC_{50}) reduced the fEPSP slope by 53.8 ± 2.6 % in control conditions and had similar effects (53.5 ± 3 % *n* = 4) in the presence of 100 nM TQ (Fig 2C, D). This shows that blocking GIRK channels has little effect on the inhibitory effect of adenosine on basal synaptic transmission in CA1.

In contrast to CA1, fEPSP slope was significantly (P=0.011) enhanced by TQ in area CA2 (29.1 ± 14.8 % increase, *n* = 8), an effect which was reversible on wash (Fig. 2E, F). There was no significant (P = 0.85) effect on the paired pulse ratio (1.65 ± 0.1 vs 1.66 ± 0.07, interval 50 ms, *n* = 8) suggesting little effect of TQ on release probability. Surprisingly, TQ also had no significant effect on the amplitude of the presynaptic fibre volley suggesting that the effects are postsynaptic. Blocking of A_1Rs (2 μM 8-CPT) also markedly enhanced fEPSP slope in CA2 (30 ± 7 %, *n* = 5, Fig 2E, F) consistent with previous reports (Simons et al 2011; Munoz and Solis 2018) of an increased A_1R tone in CA2. To test whether the

effects of TQ on fEPSP slope were only the result of blocking the GIRK channels activated by A_1Rs, TQ was applied after A_1Rs had been blocked by 8CPT (following 8CPT application, the stimulus strength was reduced so that fEPSPs had a similar slope to control). Following block of A_1Rs, TQ (100 nM) no longer enhanced fEPSP slope (Fig. 2G, H, *n* = 4) consistent with the GIRK channels being primarily activated by A_1Rs. The effects of TQ were also measured on the inhibitory effects of exogenous adenosine on synaptic transmission in CA2. Application of 20 μM adenosine reduced the fEPSP slope by 69.2 ± 2.2 % in control conditions and reduced fEPSP slope by a similar amount (69.5 ± 3.2 %, *n* = 4 slices) in the presence of 100 nM TQ (Fig 2I, J). Thus the blocking of GIRK channels had little effect on the inhibitory effect of adenosine on synaptic transmission in CA2 like that also observed in CA1.An explanation for why TQ does not affect the inhibitory actions of exogenous adenosine remains unclear.

3.3 Tertiapin-Q increases the frequency of spontaneous activity in hippocampus from young mice.

To examine the actions of TQ on spontaneous network activity, we perfused hippocampal slices with aCSF which contained no Mg^{2+} and had an elevated K^+ concentration (6 mM). This reliably induced spontaneous activity recorded in area CA1 (mean frequency of spontaneous events 0.057 ± 0.012 Hz, *n* = 20 slices, ranging from 1 burst (or population spike) every 3 s to 1 event every 70 s. The form of spontaneous activity ranged from continuous low-rate population spike-like activity (interictal-like, Fig. 3A) to isolated bursts of activity with a high frequency component (seizure-like activity Fig. 3C). For interictal-like activity, application of TQ (100 nM) increased the frequency (the mean interval between events was reduced from 18.4 ± 3.4 s to 10.7 ± 2.2 s, *n* = 15 out of 20 slices, P= 0.002, Fig. 3A, B). This effect of TQ was partially reversible upon wash (interval 15.8 ± 5 s). The increase in frequency was often accompanied by a decrease in spike amplitude. For activity which consisted of isolated bursts (seizure activity), TQ also reduced the interval between

the bursts (32 ± 5 %, *n* = 5 out of 7 slices) and could also increase burst duration (for example see Fig. 3C) although this was not always observed.

The GIRK channels that are open during network activity could stem from the activation of a number of different metabotropic receptors including A_1R, $GABA_B$, mGluRs etc. Probably all of these receptors will be activated during seizure activity. We assessed the role of A_1Rs in controlling spontaneous network activity by applying the A_1R antagonist 8-CPT (2 μM). The frequency of activity was markedly increased by 225 ± 20 % (*n* = 5, Fig. 3D) which was significantly larger than the effect of TQ (36.7 ± 4.7 %). In contrast block of $GABA_B$ receptors (CGP35348 10 μM) had a much smaller effect on the frequency of activity (32.5 ± 5 % decrease in inter-event interval, *n* = 6 slices, Fig 3E). We then assessed the actions of TQ on seizure activity when either $GABA_B$ or A_1R were blocked. The effects of TQ were not changed when seizures were induced in the presence of the $GABA_B$ receptor antagonist CGP35348 (10 μM, *n* = 4, 31.5 ± 3 % fall in event interval, Fig 3F) but the effects were abolished in the presence of 8CPT (2 μM*, n* = 3 Fig. 3G).

To precisely determine the contribution of each species of GPCR to the activation of GIRK channels during seizures requires the application of multiple receptor antagonists. Thus we took a different approach and assessed the role that GIRK channels play in the supressing actions that exogenous adenosine has on network activity (Fig 3H, I). A low concentration of adenosine (10 μM) was applied during seizure activity and washed. Adenosine was then applied in the presence of TQ (100 nM) and following the wash of TQ applied again. In 6 slices, adenosine (10 μM) virtually abolished all network activity (reduced from 123 ± 4 events in 5 minutes to 3 ± 5 events after adenosine application) whereas in the presence of TQ activity persisted (45 ± 6 events in 5 minutes), although the level of activity was still reduced compared to control (Fig 3H, I). When TQ was washed the supressing effects of adenosine were almost recovered (15 ± 3 events in 5 minutes, Fig 3H, I). Thus GIRK channels do play a role in the actions of adenosine in supressing this form of spontaneous network activity.

These experiments were carried out in slices from young mice and there maybe differences in GIRK channels and adenosine signalling during postnatal development. Thus we repeated the experiments on spontaneous activity in slices from older mice (2-3 months). Just as with slices from young mice, TQ (100 nM) increased the frequency of population spikes in interictal-like activity (mean increase 32.8 ± 6 %, n = *6* slices) and reduced their amplitude (Fig 3J). TQ application reduced the interval between bursts in seizure-like activity (Fig 3K). Thus the effects of TQ were very similar to that observed in slices from younger mice.

3.4 Whole cell patch clamp recording from CA1 neurons

To investigate the actions of TQ on spontaneous activity in more detail, whole cell patch clamp recordings were made from CA1 pyramidal neurons in aCSF with zero Mg^{2+} and 6 mM K^+ in slices from young mice. Slices were transferred to the recording chamber in zero Mg^{2+} and 6 mM K^+ aCSF and incubated for at least 15 minutes before recording to allow network activity to reach steady state. In this solution, CA1 pyramidal neurons had a mean resting potential of -55 ± 3 mV (*n* = 30). Many neurons (18 out of 30) showed a pattern of short-lived depolarisations (frequency 0.4 ± 3 Hz, amplitude 3-10 mV, mean 7.5 ± 3 mV) with superimposed action potentials (Fig. 4A). These depolarisations probably arise from the synaptic activation of NMDA receptors. A small number of CA1 neurons were quiescent (n = 5, Fig. 4B) and some neurons showed short bursts of activity with a small high frequency component (7 neurons). We did not observe clear seizure-like bursts in the whole cell recording experiments unlike those with field recording. Application of TQ (100 nM) depolarised some CA1 neurons (5.5 ± 0.7 mV, 10 out of 30, Fig. 4B) but many neurons showed no change in membrane potential. However even in those pyramidal cells in which TQ did not change the membrane potential, TQ increased the frequency of spontaneous activity. There was a significant ($P<0.001$) increase in the frequency of depolarisations leading to increased action potential firing (from 0.4 ± 0.5 to 1.1 ± 2 Hz). This stemmed from

an increase in the frequency of depolarising events and an increase in the amplitude of events (10.5 ± 2 mV, Fig. 4C).

3.5 Tertiapin-Q has a markedly greater effect on electrically-induced seizure activity in CA2 vs CA1

To compare the effects that GIRK channel activation has on seizure activity in CA1 versus that in CA2, seizure activity was electrically stimulated. By positioning the recording and stimulating electrodes as for fEPSP recording we could localise stimulated network activity in CA1 and CA2. By using electrical stimulation we have precise control over the strength and temporal pattern of activity. Bursts of activity were evoked every 15 minutes by a 2 second 60 Hz stimulation in aCSF which contained zero Mg^{2+} (Etherington and Frenguelli, 2004). At this interval, the duration of evoked bursts was consistent. With shorter intervals the bursts got shorter and shorter in duration presumably as adenosine was accumulating in the extracellular space. This protocol produces reliable activity in CA1 following the stimulus with little or no spontaneous activity between stimulations (Etherington and Frenguelli, 2004). Stimulation induced significantly (P = 0.012) more spikes in CA1 (17.5 ± 7, Fig. 5A, B) than in CA2 (5.3 ± 3.2, Fig 5C, D). Application of TQ (100 nM) significantly increased the number of spikes per stimulation in CA1 (mean increase of 33.8 ± 5 %, from 17.5 ± 7 to 26 ± 5 spikes, P = 0.025, *n* =10, Fig 5A,B) and in CA2 (mean increase of 468.2 ± 77 % from 5.3 ± 3.2 to 42.5 ± 8, n = 8, P=0.0065, Fig. 5C, D). However TQ had a significantly greater effect in CA2 (two way ANOVA, P = 0.001, Fig. 5E). TQ also greatly increased the amplitude of activity in CA2 (233 ± 113% increase in peak amplitude of rectified bursts Fig. 5F) with little effect on the amplitude of activity in CA1 (4.6 ± 1.3 %, Fig. 5F). Thus it appears that there are greater numbers of GIRK channels open in CA2 compared to CA1 which supresses the induction of network activity in this region of the hippocampus. TQ also reliably (*n* =10 out of 10 slices) induced spontaneous activity which was absent in control.

3.6 Investigating whether GIRK channels can influence the spread of seizure activity

To investigate whether GIRK channels play a role in the spatial spread of spontaneous seizure activity across tissue, we placed extracellular recording electrodes in the neocortex and in the hippocampus within the same slice (Fig 6A) and applied zero Mg^{2+} 6 mM K^+ aCSF. We then investigated whether TQ influenced activity in the hippocampus and in the neocortex. In slices in which activity appeared coupled across the neocortex and hippocampus (Fig 6B, D), TQ increased the frequency of activity in both the hippocampus and in the neocortex (Fig 6E, *n* = 5 slices). However in slices in which activity in the neocortex appeared temporally independent of that in the hippocampus (Fig 6C,D) TQ only increased the frequency of activity in the hippocampus (Fig 6F). This suggests that the increases in the frequency of activity in the neocortex stems from an increase in the hippocampus. In those slices in which activity was couple between the neocortex and hippocampus were connected we investigated whether TQ increased the spread of electrically stimulated activity in the hippocampus. Although TQ increased the number of spikes induced in the hippocampus (Fig 6 E) we did not observe any spread of activity into the neocortex following TQ application (*n* = 6 slices). This data suggests that TQ has larger effects in the hippocampus than the neocortex.

4. Discussion

We have shown that approximately half of the membrane potential hyperpolarisation produced by adenosine in CA1 and CA2 pyramidal cells is blocked by tertiapin-Q (TQ, 100 nM) and thus results from GIRK channel activation. Similar effects have been observed in other studies, for example in retinal ganglion cells TQ (30 nM) blocks ~ 56 % of the NECA-induced current (Clark et al 2009). The inability of TQ to block all of the A_1R-mediated hyperpolarisation/outward current indicates that A_1Rs open other K^+ channels as well as

GIRK channels. In retinal gangion cells for example, A_1Rs also activate small conductance calcium activated K^+ channels (Clark et al., 2009) and in the olfactory bulb A_1Rs activate background 2 pore K^+ channels (Rotermund et al., 2018). This activation of multiple K^+ channels appears to be a common phenomenon across GPCRs, with other metabotropic receptors such as $GABA_B$ receptors activating additional K^+ channels as well as GIRK channels (Breton and Stuart, 2017).

We found TQ had no effect on the resting potential of either CA1 or CA2 pyramidal neurons under basal conditions and only depolarised the membrane potential of a subset of CA1 neurons during seizure activity. Kim and Johnson (2015) found that CA1 neurons were depolarised by TQ (4-5 mV) in dorsal hippocampal slices from 11-13 wk old rats. Takaigawa and Alzheimer (2002) reported that there is a standing inwardly rectifying K^+ current in CA1 neurons which is blocked by TQ again in rat hippocampal slices (2-3 week old). The lack of effect of TQ on resting potential that we observed may reflect a species difference. Also our patch clamp experiments were carried out in slices from immature animals (postnatal days 12-18) where the A_1R tone is low (Kerr et al., 2013).

The application of TQ had no significant effect on the initial slope or paired pulse ratio of fEPSPs recorded in CA1. Antagonism of A_1Rs (with 8-CPT) only increased fEPSP slope by ~ 10 %. In previous studies, groups have reported an increase in fEPSP slope of 28 % (Diogenes et al 2014) and 22 % (Sandau et al., 2016) although both these studies were carried out in slices from older mice. This contrasts with fEPSPs recorded in CA2, where both TQ (28 % increase) and 8CPT (30 % increase) significantly enhanced fEPSP slope. The effects of TQ in CA2 were abolished when A_1Rs were blocked with 8-CPT. Thus TQ enhances transmission by blocking A_1R-activated GIRK channels. This difference between CA1 and CA2 is consistent with previous reports of greater basal activation of A_1R pathways in CA2 (Munoz and Solis, 2018; Simons et al., 2011). It has been suggested by Munoz and Solis (2018) that this greater activity is not the result of a greater extracellular concentration of adenosine in CA2 but instead results from tighter coupling between receptors and

downstream pathways. In about half of the slices tested, the magnitude of the actions of TQ on fEPSP slope were of a similar magnitude to the effects of blocking A_1Rs (as illustrated in Fig 2C). This suggests that all the actions of endogenous A_1R activation on fEPSP slope could be accounted for by the opening of GIRK channels. Interestingly, TQ increased fEPSP slope in CA2 without changing either the paired pulse ratio or the amplitude of the presynaptic fibre volley. This suggests that the mechanism for the increase in fEPSP slope occurs postsynaptically. Luscher et al (1997) showed that deletion of GIRK2 abolishes the outward current induced by metabotropic receptors such as A_1R but had no effect on the presynaptic inhibition of transmitter release. Thus the effects of GIRK channels are only postsynaptic. This is supported by Takigawa and Alzhiemer (2002) who showed that block of GIRK channels (with TQ), enhances the amplitude of currents induced by puffing glutamate onto rat hippocampal pyramidal cells. The mechanism for this enhancement is the removal of the shunting of the synaptic current as it propagates from the dendrite to the soma (Takigawa and Alzheimer, 2002).

It is unclear why TQ enhances synaptic transmission to CA2 neurons but does not reduce the inhibitory effects of applied adenosine. The lack of effect of TQ on exogenous adenosine suggests that all its inhibitory effects are presynaptic and thus it has different effects to endogenous adenosine.

It was reported by Simons et al (2012) that caffeine and A_1 receptor antagonists produce long lasting enhancement of synaptic transmission in CA2 as a result of AMPA receptor insertion. In Simons et al (2012) blocking of A_1 receptors produced a very much larger enhancement of fEPSPs than we observed. We did not try and wash the 8-CPT that we applied so we cannot know whether or not the effects we observed persisted or waned and thus it is unclear if AMPA receptor insertion contributes to the observed effects

4.1 Role of GIRK channels in controlling spontaneous seizure activity

The inhibition of GIRK channels, with TQ, increased the frequency of spontaneous network activity induced by zero Mg^{2+} high K^+ aCSF. In this model, the elevated K^+ concentration will depolarise neurons increasing activity. Although we applied the TQ for short periods (5-15 mins) we cannot exclude that some of the observed effects are due to the block of BK channels as well as GIRK channels (Kanjhan et al 2005).The effects of TQ were not large, with the frequency of spontaneous activity (both interictal and seizure-like) increased by ~ 30 %.In some slices the duration of bursts of activity was also increased but this was variable. The effects of blocking GIRK channels were relatively minor when compared to the effects of blocking A_1Rs (compare Fig 3A to Fig 3D). This raises two possibilities either the inhibition of synaptic transmission is more important than the membrane potential hyperpolarisation or that K^+ channels, other than GIRK, activated by A_1Rs play a more major role in controlling activity. It can be argued that the effects of TQ are an underestimate of the role of GIRK channels as any increase in activity will potentially lead to greater adenosine release which will feedback and inhibit activity. By applying TQ during seizure activity, all GIRK channels will be inhibited with no selectivity for those GIRK channels activated by A_1Rs. We showed that blocking $GABA_B$ receptors had a much smaller effect than blocking A_1Rs but other metabotropic receptors will also be activated during seizure activity. To directly assess the role of GIRK channels in the supressing effects of A_1R activation we applied low concentrations of adenosine and measured the effects of TQ. We chose this concentration of adenosine as it is around the IC_{50} and thus will not completely block synaptic transmission. We found that TQ blunted the effects of adenosine allowing activity to persist. Thus the effects of TQ may be dependent on the concentration of adenosine in the tissue and whether the effects on seizure activity is dominated by the presynaptic inhibition of transmitter release.

From whole cell patch clamp recordings it was found that TQ could enhance the frequency of spontaneous activity without changing the membrane potential of CA1 pyramidal cells. This increase in the frequency of CA1 neuron firing stemmed at least in part from an

increase in the amplitude of depolarising events which may stem from enhanced propagation of synaptic currents to the soma and initial segment (Takigawa and Alzheimer, 2002) or upstream changes in CA3 neurons. The removal of Ca^{2+} ions from aCSF produces similar activity in CA1 neurons to perfusion with Mg^{2+} free, 6 mM K^{+} aCSF (short depolarisations and superimposed action potentials, Diez et al., 2017). Here the block of A_1Rs produced a large depolarisation of membrane potential, although the role of GIRK channels is unclear. TQ had a larger effect on activity recorded with patch clamp recording versus that recorded with extracellular recording. This could stem from a greater extracellular concentration of adenosine in slices which are used for patch clamp recording as they sit on a glass coverslip and are not on a raised grid like the extracellular recorded slices (although this has not been shown).

By recording from the neocortex and hippocampus simultaneously in the same slice we could assess the role of GIRK channels in these two brain regions. We found that GIRK channels play a role in controlling activity the hippocampus but appear to play less of a role in the neocortex. Thus TQ had no significant effect on the activity in isolated neocortex, but enhanced activity when the hippocampus was coupled to the neocortex. It appears that A_1 receptor activation has much less effect on the membrane potential of pyramidal cells in the neocortex vs those in the hippocampus. It has also been shown that $GABA_B$ receptors do not couple to GIRK channels in the neocortex but do in the hippocampus (Breton and Stuart 2017). A similar phenomenon may occur with A_1 receptors.

4.2 Role of GIRK channels in controlling electrically-stimulated network activity

By electrically stimulating epileptiform activity it was possible to measure the activity induced in CA1 vs CA2. This was carried out in aCSF with zero Mg^{2+} and there was little or no spontaneous activity and thus is well controlled. TQ increased the duration of bursts in both CA1 and CA2, although TQ had a much larger effect on burst duration and spike amplitude

in CA2. Each burst of activity will evoke adenosine release (reviewed in Frenguelli and Wall, 2015) which will inhibit synaptic transmission and hyperpolarise neurons. When the inhibition outweighs excitation then activity will be terminated. In CA1, the block of GIRK channels shifts the balance so that activity persists longer. Presumably the same thing occurs in CA2 but the greater A_1R activation leads to shorter bursts and a greater effect of TQ. There is probably greater A_1R activation between bursts. It is also possible that GIRK channels play a greater role in the supressing effects of adenosine in CA2 versus CA1.This lack of excitability for CA2 fits with the concept of CA2 acting as a fire break preventing the spread of seizure activity across the hippocampus. For example, temporal lobe epilepsy (TLE), is commonly associated with hippocampal sclerosis, which includes severe loss of pyramidal cells (Corsellis and Bruton, 1983) However, CA2 neurons do not often display this pathology and examination of hippocampi from patients with TLE and/or status epilepticus demonstrated that area CA2 is resistant to cell loss (Steve et al., 2014). It is thought that this resistance stems from differences in Ca^{2+} handling (Sloviter et al., 1991) combined with the greater A_1R activation. It has also been reported that there is a dense network of perineuronal nets (PNN) around pyramidal cells in CA2 which may also contribute to the resistance of CA2 neurons to damage from epileptic activity (Carstens et al 2016)

Acknowledgements

Emily Hill is an MIPTP PhD student funded by the BBSRC.

References

Boison, D., 2013. Adenosine and Seizure Termination: Endogenous Mechanisms. Epilepsy Currents 13, 35-37.

Breton, J.D., Stuart, G.J., 2017. $GABA_B$ receptors in neocortical and hippocampal pyramidal neurons are coupled to different potassium channels. Eur. J. Neurosci. 46, 2859-2866.

Carstens, K.E., Phillips, M.L., Pozzo-Miller, L., Weinberg, R.J., Dudek ,S.M., 2016 Perineuronal Nets Suppress Plasticity of Excitatory Synapses on CA2 Pyramidal Neurons. J. Neurosci.36, 6312-6320.

Chevaleyre, V., Siegelbaum, S.A., 2010. Strong CA2 pyramidal neuron synapses define a powerful disynaptic cortico-hippocampal loop. Neuron 66, 560-572.

Clark, B.D., Kurth-Nelson, Z.L., Newman, E.A., 2009. Adenosine-evoked hyperpolarization of retinal ganglion cells is mediated by G-protein-coupled inwardly rectifying K+ and small conductance Ca2+-activated K+ channel activation. J. Neurosci. 29, 11237-45.

Corsellis, J.A., Bruton, C.J., 1983. Neuropathology of status epilepticus in humans. Adv. Neurol. 34, 129–139

Diez, R., Richardson, M.J.E., Wall, M.J., 2017. Reducing Extracellular Ca_{2+} Induces Adenosine Release via Equilibrative Nucleoside Transporters to Provide Negative Feedback Control of Activity in the Hippocampus. Front. Neural Circuits 11:75. doi: 10.3389/fncir.2017.00075.

Diógenes, M.J., Neves-Tomé, R., Fucile, S., Martinello, K., Scianni, M., Theofilas, P., Lopatár, J., Ribeiro, J.A., Maggi, L., Frenguelli, B.G., Limatola, C., Boison, D., Sebastião, A.M., 2014. Homeostatic control of synaptic activity by endogenous adenosine is mediated by adenosine kinase. Cereb. Cortex. 24, 67-80.

Dunwiddie, T.V., Fredholm, B.B., 1989, Adenosine A1 receptors inhibit adenylate cyclase activity and neurotransmitter release and hyperpolarize pyramidal neurons in rat hippocampus. J. Pharmacol. Exp. Ther. 249, 31-7.

During, M.J., Spencer, D.D., 1992. Adenosine: A potential mediator of seizure arrest and postictal refractoriness. Ann. Neurol*. 32,* 618–624.

Etherington, L.A., Frenguelli, B.G., 2004. Endogenous adenosine modulates epileptiform activity in rat hippocampus in a receptor subtype-dependent manner. Eur. J. Neurosci. 19, 2539-50.

Frenguelli, B.G., Wall, M.J., 2016. Combined electrophysiological and biosensor approaches to study purinergic regulation of epileptiform activity in cortical tissue. J. Neurosci. Methods 260, 202-214.

Gauldie, J., Hanson, J.M., Rumjanek, F.D., Shipolini, R.A., Vernon, C.A., 1976. The peptide components of bee venom. Eur. J. Biochem. 61, 369-76.

Jin. W., Lu, Z., 1998. A novel high-affinity inhibitor for inward-rectifier K+ channels. Biochemistry 37, 13291-9.

Jin, W., Lu, Z., 1999. Synthesis of a stable form of tertiapin: a high-affinity inhibitor for inward-rectifier K+ channels. Biochemistry 38, 14286-93.

Kanjhan, R., Coulson, E.J., Adams, D.J., Bellingham, M.C., 2005. Tertiapin-Q blocks recombinant and native large conductance K+ channels in a use-dependent manner. J. Pharmacol. Exp. Ther. 314, 1353-61.

Kerr, M.I., Wall, M.J., Richardson, M.J., 2013. Adenosine A1 receptor activation mediates the developmental shift at layer 5 pyramidal cell synapses and is a determinant of mature synaptic strength. J. Physiol. 591, 3371-80.

Kim, C.S., Johnston, D., 2015, A1 adenosine receptor-mediated GIRK channels contribute to the resting conductance of CA1 neurons in the dorsal hippocampus. J. Neurophysiol. 113, 2511-23.

Klyuch, B.P., Dale, N., Wall, M.J., 2012. Deletion of ecto-5'-nucleotidase (CD73) reveals direct action potential-dependent adenosine release. J. Neurosci. 32, 3842-7.

Kobayashi, T., Ikeda, K., 2006. G protein-activated inwardly rectifying potassium channels as potential therapeutic targets. Curr. Pharm. Des. 12, 4513-23.

Lüscher, C., Jan, L.Y., Stoffel, M., Malenka, R.C., Nicoll, R.A., 1997. G protein-coupled inwardly rectifying K+ channels (GIRKs) mediate postsynaptic but not presynaptic transmitter actions in hippocampal neurons. Neuron 19, 687-95.

Muñoz, M.D., Solís, J.M., 2019. Characterisation of the mechanisms underlying the special sensitivity of the CA2 hippocampal area to adenosine receptor antagonists. Neuropharm 144, 9-18.

Newman, E.A., 2004. Glial modulation of synaptic transmission in the retina. Glia. 47, 268-74.

Ochiishi, T., Saitoh, Y., Yukawa, A., Saji, M., Ren, Y., Shirao, T., Miyamoto, H., Nakata, H., Sekino, Y., 1999. High level of adenosine A1 receptor-like immunoreactivity in the CA2/CA3a region of the adult rat hippocampus. Neuroscience 93, 955-67.

Rotermund. N., Winandy, S., Fischer, T., Schulz, K., Fregin, T., Alstedt, N., Buchta, M., Bartels, J., Carlström, M., Lohr, C., Hirnet, D., 2018. Adenosine A_1 receptor activates background potassium channels and modulates information processing in olfactory bulb mitral cells. J. Physiol. 596, 717-733.

Pankratov, Y., Lalo, U., Verkhratsky, A., North, R.A., 2007. Quantal release of ATP in mouse cortex. J. Gen. Physiol. 129, 257-65.

Sandau, U.S., Colino-Oliveira, M., Jones, A., Saleumvong, B., Coffman, S.Q., Liu, L., Miranda-Lourenço, C., Palminha, C., Batalha, V.L., Xu, Y., Huo, Y., Dióge, J. 2016. Adenosine Kinase Deficiency in the Brain Results in Maladaptive Synaptic Plasticity. J. Neurosci. 36, 12117-12128.

Sickmann, T., Alzheimer, C., 2003. Short-term desensitization of G-protein-activated, inwardly rectifying K+ (GIRK) currents in pyramidal neurons of rat neocortex. J. Neurophysiol. 90, 2494-503.

Simons, S.B., Caruana, D.A., Zhao, M., Dudek, S.M., 2011. Caffeine-induced synaptic potentiation in hippocampal CA2 neurons. Nat. Neurosci. 15, 23-5.

Sloviter, R.S., Sollas, A.L., Barbaro, N.M., Laxer, K.D., (1991) Calcium-binding protein (calbindin-D28K) and parvalbumin immunocytochemistry in the normal and epileptic human hippocampus. J. Comp. Neurol. 308, 381–396.

Steve, T.A., Jirsch, J.D., Gross, D.W., 2014. Quantification of subfield pathology in hippocampal sclerosis: a systematic review and meta-analysis. Epilepsy Res. 108, 1279–1285.

Takigawa, T., Alzheimer, C., 2002. Phasic and tonic attenuation of EPSPs by inward rectifier K+ channels in rat hippocampal pyramidal cells. J. Physiol. 539, 67-75.

Thompson, S.M., Haas, H.L., Gähwiler, B.H., 1992. Comparison of the actions of adenosine at pre- and postsynaptic receptors in the rat hippocampus in vitro. J. Physiol. 451, 347-63.

Trusell, L. O., JACKSON, M. B., 1985. Adenosine-activated potassium conductance in cultured striatal neurons. Proc. Natl. Acad. Sci. U.S.A. 82, 4857-4861.

Trusell, L. O., Jackson, M. B., 1987. Dependence of an adenosine-activated potassium current on a GTP-binding protein in mammalian central neurons. J. Neurosci. 7, 3306-3416.

Wall, M.J., Dale, N., 2013. Neuronal transporter and astrocytic ATP exocytosis underlie activity-dependent adenosine release in the hippocampus. J. Physiol. 591, 3853-71.

Wall, M.J., Richardson, M.J., 2015. Localized adenosine signaling provides fine-tuned negative feedback over a wide dynamic range of neocortical network activities. J. Neurophysiol. 113, 871-82.

Wall, M.J., Collins, D.R., Chery, S.L., Allen, Z.D., Pastuzyn, E.D., George, A.J., Nikolova, V.D., Moy, S.S., Philpot, B.D., Shepherd, J.D., Müller, J., Ehlers, M.D., Mabb, A.M., Corrêa, S.A.L., 2018. The Temporal Dynamics of Arc Expression Regulate Cognitive Flexibility. Neuron. 98, 1124-1132.

Zhang, Y., Huang, Y., Wang, G., Wang, X., Wang, Y., 2017. Inhibition of 17-beta-estradiol on neuronal excitability via enhancing GIRK1-mediated inwardly rectifying potassium currents and GIRK1 expression. J. Neurol. Sci. 375, 335–341.

Legends

Fig. 1. Tertiapin-Q (TQ) reduces the membrane potential hyperpolarisation produced by adenosine in CA1 and CA2 pyramidal neurons. A**,** Characteristic current-voltage relationships for a CA1 and CA2 pyramidal cell (100 pA steps from -300 pA). B, TQ (100 nM) had no effect on the membrane potential of either a CA1 or CA2 pyramidal cell. C, membrane potential traces recorded from CA1 and CA2 pyramidal neurons. The hyperpolarisation produced by adenosine (100 μM) is reduced (~50 %) by pre-incubation with TQ (100 nM). D, Graph summarising data from CA1 and CA2 pyramidal cells showing effects of TQ on membrane potential hyperpolarisation. Points are data from single experiments, bars show mean and SEM.

Fig. 2. Tertiapin-Q (TQ) has little effect on synaptic transmission in CA1 but can enhance synaptic transmission in CA2. A, Graph plotting fEPSP slope (normalised to baseline) for a single recording from CA1. Neither tertiapin-Q (TQ, 100 nM) nor 8-CPT (2 μM) had a significant effect on fEPSP slope. Inset, fEPSP waveform averages in control, TQ, wash and in 8-CPT. B, Graph summarising mean data from 5-12 slices. C, Graph plotting fEPSP slope (normalised to baseline) for a single recording from CA1. Application of adenosine (20 μM) had the same inhibitory effect on fEPSP slope in TQ (100 nM) compared to control. D, Graph summarising mean data from 4 slices. E, Graph plotting fEPSP slope (normalised to baseline) for a single recording from CA2. TQ (100 nM) reversibly increases fEPSP slope (~ 40 %) and 8-CPT also increases fEPSP slope (~ 40 %). Inset, fEPSP waveform averages in control, TQ, wash and in 8-CPT. F, Graph summarising mean data from 8 slices. G, Graph plotting fEPSP slope (normalised to baseline) for a single recording from CA2 . TQ (100 nM) increased fEPSP slope in control but had no effect after A_1Rs were blocked by 8 CPT (2 μM). The stimulus strength was reduced after the application of 8CPT so that fEPSPs had a similar slope as in control. H, Graph summarising mean data from 5-12 slices. I, Graph

plotting fEPSP slope (normalised to baseline) for a single recording from CA2. Application of adenosine (20 μM) had the same inhibitory effect on fEPSP slope in TQ (100 nM) compared to control. J, Graph summarising mean data from 4 slices.

Fig. 3. Inhibition of GIRK channels enhances spontaneous network activity recorded in CA1. A, Example extracellular recording of spontaneous network activity where events were continuous (interictal-like activity) and application of tertiapin-Q (TQ, 100 nM) reduced the interval between events. B, Summary of data from 10 slices. C, Example where network activity consisted of separated bursts of activity (seizure-like activity). Application of TQ (100 nM) reduced the interval between bursts, increased the duration of bursts and increased spike amplitude. D, Example extracellular trace showing that blocking A_1Rs (8CPT 2 μM) has a marked effect on the frequency of spontaneous activity. E, Example extracellular trace illustrating the small effect of blocking $GABA_B$ receptors on the frequency and amplitude of activity (10 μM CGP35348). F, Application of TQ (100 nM) still reduced the interval between events when $GABA_B$ receptors were blocked (10 μM CGP35348). G, TQ (100 nM) has little effect on the frequency of activity when A_1 receptors were blocked (10 μM 8CPT). H, Example extracellular traces recorded from the same slice. Application of adenosine (10 μM) abolished activity, whereas activity persisted when adenosine (10 μM) was applied in the presence of TQ (100 nM). The effects of adenosine were partially recovered when TQ was washed. I, Data summarised from 6 slices. The effects of adenosine were significantly (P= 0.001) reduced when it was applied in the presence of TQ. J, Example extracellular recording of spontaneous network activity from slices from a P42 mouse where events were continuous (interictal-like activity) and application of TQ (100 nM) reduced the interval between events and also reduced event amplitude. K, Example where network activity consisted of separated bursts of activity (seizure-like activity) recorded from a P38 mouse. Application of TQ, (100 nM) reduced the interval between bursts.

Spontaneous activity was induced with aCSF which contained no Mg^{2+} and with elevated K^{+} (6 mM).

Fig. 4. Tertiapin-Q (TQ) can increase network activity without changing the membrane potential of CA1 pyramidal neurons. A, Example recordings of the membrane potential from a CA1 pyramidal cell. In control the resting potential was ~ -53 mV with short duration depolarisations and superimposed action potentials. Inset, single example of a short depolarisation. Application of TQ (100 nM) increased the frequency of depolarisations without changing the resting membrane potential. B, Example of a quiescent pyramidal cell (resting potential -56 mV). Application of TQ (100 nM) reversibly depolarised the membrane potential leading to action potential firing. C, Example recordings of the membrane potential from a CA1 pyramidal cell. The action potentials are truncated at -20 mV to illustrate the increase in the amplitude of the depolarising events that occur in TQ (100 nM). All of the recordings in this figure were carried out in aCSF with zero $Mg2^{+}$ and with 6 mM $K^{+,}$ with slices pre-incubated in the solution for at least 15 minutes before recording so that activity could reach a steady state.

Fig. 5. Blocking GIRK channels enhances electrically-stimulated seizure activity to a greater extent in CA2 compared to CA1 in the hippocampus. A, Single examples of electrically-stimulated (2 s, 60 Hz, zero Mg^{2+} aCSF) bursts of network activity recorded in CA1 in control and in the presence of tertiapin-Q (TQ, 100 nM). TQ increased the duration of the activity (number of spikes evoked). B, Graph plotting the mean number of spikes per burst (induced in CA1) in control and in TQ (100 nM) for 10 slices. C, Single examples of electrically-stimulated bursts of network activity recorded in CA2 in control and in the presence of TQ (100 nM). TQ increased the number of spikes from 2 to 15 and also markedly increased spike amplitude D, graph plotting the mean number of spikes per burst (induced in CA2) in

control and in TQ (100 nM). E, Graph plotting the mean percentage increase in spike number per burst after TQ application in CA1 and CA2. F, Graph plotting the mean increase in peak spike amplitude induced by TQ in CA1 and in CA2. The inset shows example activity traces in control (top) and in TQ (bottom) induced in CA to illustrate the marked increase in amplitude and frequency.

Fig 6. Effects of tertiapin-Q (TQ) on activity recorded in the hippocampus and neocortex in the same slice. A, image of brain slice with positioning of recordings and stimulating electrodes. The box shows the somatosensory cortex (hind limb). B, Example extracellular recordings of spontaneous network activity from the neocortex and hippocampus in the same slice where activity is temporally correlated. C, Example extracellular recordings of spontaneous network activity from the neocortex and hippocampus in the same slice where activity is not correlated. D, Graph plotting the correlation between waveforms in the neocortex and hippocampus from experiments in B and C. E, Graphs of instantaneous frequency (the line is running average of 10 events) plotted against event number (for the experiment in A). Application of TQ (100 nM) increased the frequency of activity in both the hippocampus and the neocortex. F, E, Graphs of instantaneous frequency (the lines/points are running averages of 10 events) plotted against event number (for the same experiment in B). Application of TQ (100 nM) increased the frequency of activity in the hippocampus but not in the neocortex. G, Activity was stimulated (at *) with an electrode placed in the hippocampus and recorded in CA1 and in the somatosensory cortex. Although TQ (100 nM) increased the number of events stimulated in the hippocampus it did not increase the spread into the neocortex.

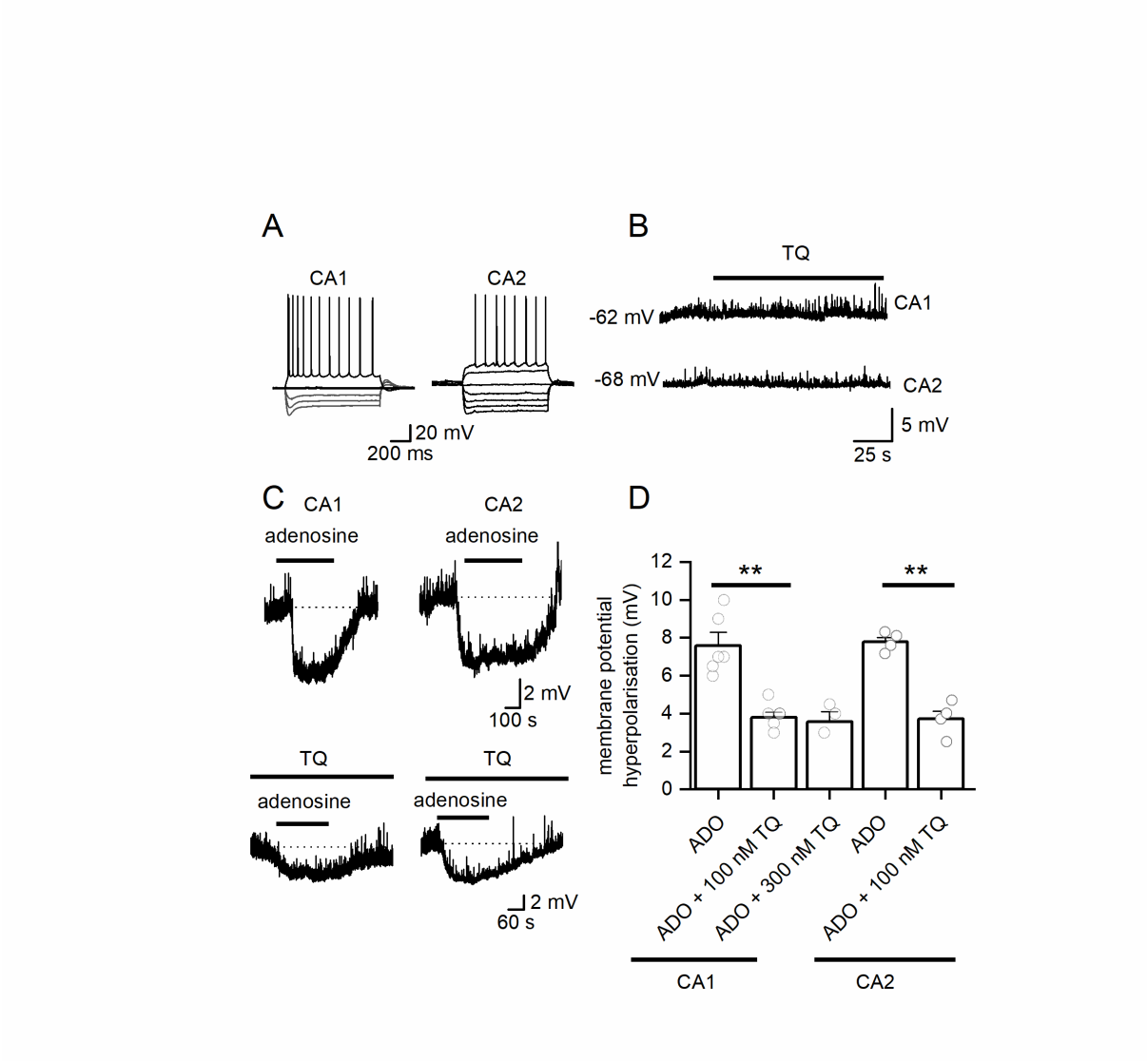
A
CA1
CA2
20 mV
200 ms
B
TQ
-62 mV
CA1
-68 mV
CA2
5 mV
25 s
C
CA1
CA2
adenosine
adenosine
2 mV
100 s
TQ
TQ
adenosine
adenosine
2 mV
60 s
D
membrane potential hyperpolarisation (mV)
12
10
8
6
4
2
0
**
**
ADO
ADO + 100 nM TQ
ADO + 300 nM TQ
ADO
ADO + 100 nM TQ
CA1
CA2

Figure 1

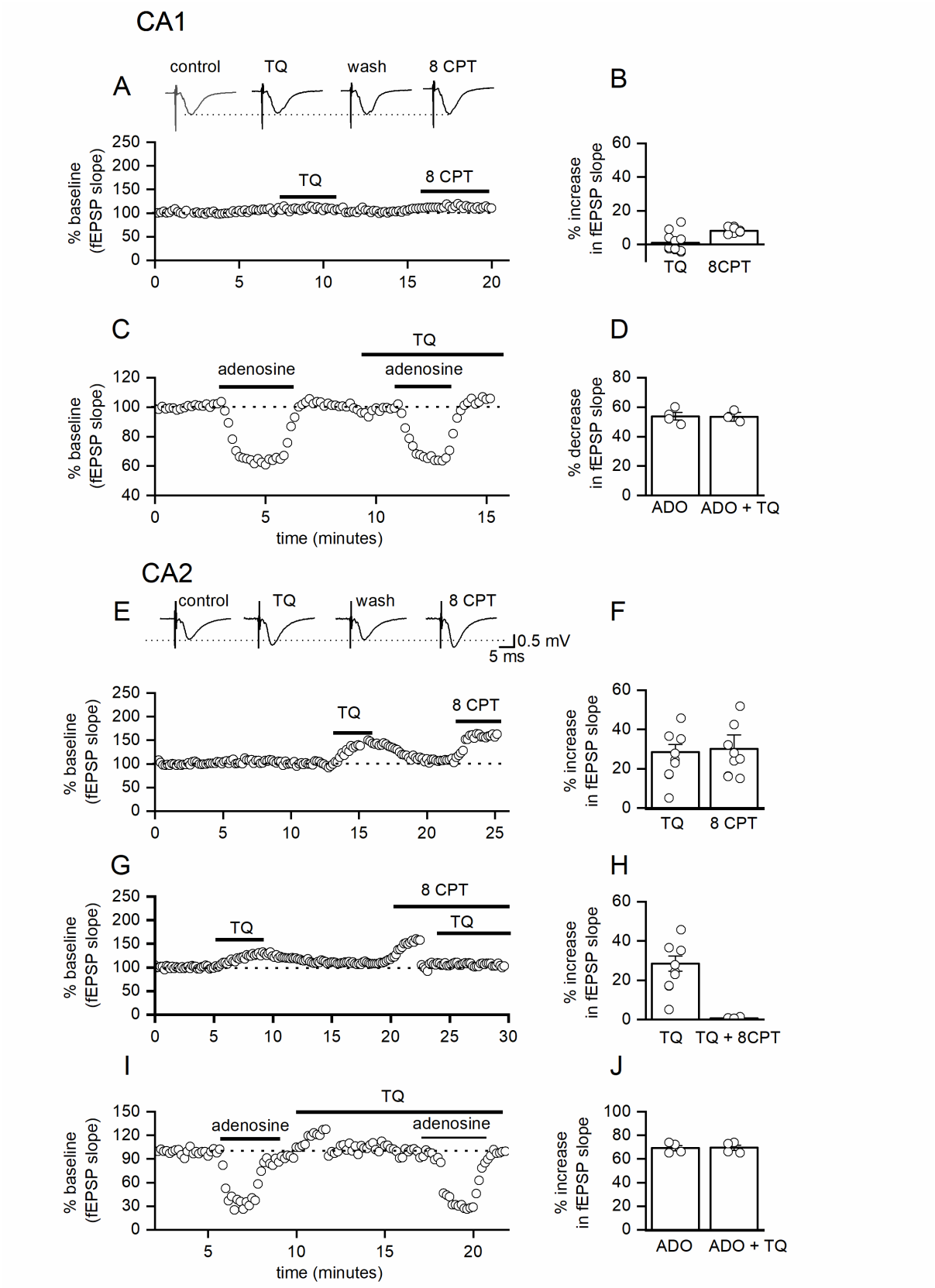
CA1
A
control
TQ
wash
8 CPT
% baseline (fEPSP slope)
TQ
8 CPT
B
% increase in fEPSP slope
TQ
8CPT
C
adenosine
adenosine
TQ
time (minutes)
D
% decrease in fEPSP slope
ADO
ADO + TQ
CA2
E
0.5 mV
5 ms
F
G
H
TQ + 8CPT
I
J

Figure 2.

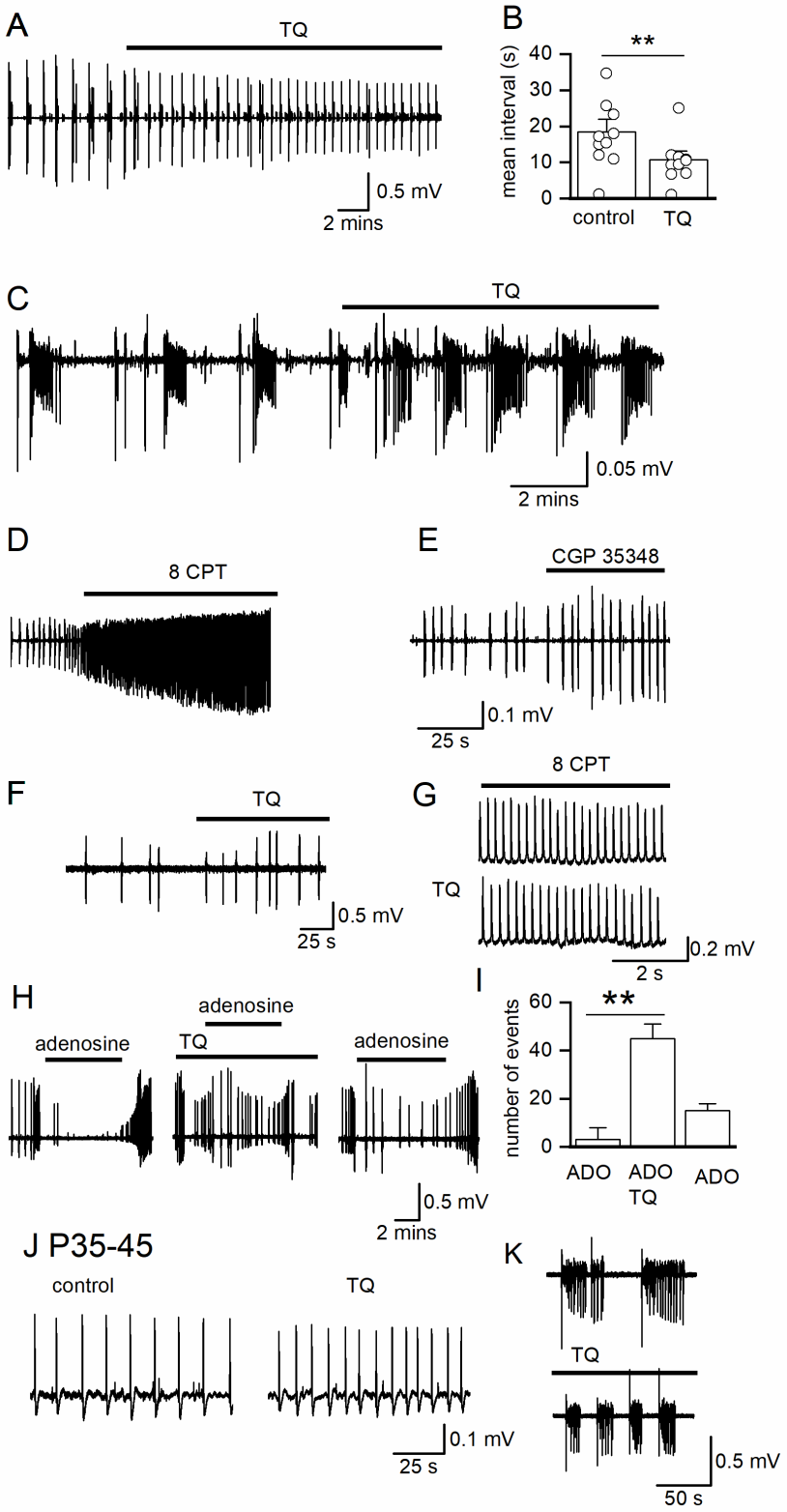
A
TQ
0.5 mV
2 mins
B
**
mean interval (s)
40
30
20
10
0
control
TQ
C
TQ
0.05 mV
2 mins
D
8 CPT
E
CGP 35348
0.1 mV
25 s
F
TQ
0.5 mV
25 s
G
8 CPT
TQ
0.2 mV
2 s
H
adenosine
adenosine
TQ
adenosine
0.5 mV
2 mins
I
**
number of events
60
40
20
0
ADO
ADO
TQ
ADO
J P35-45
control
TQ
0.1 mV
25 s
K
TQ
0.5 mV
50 s

Figure 3

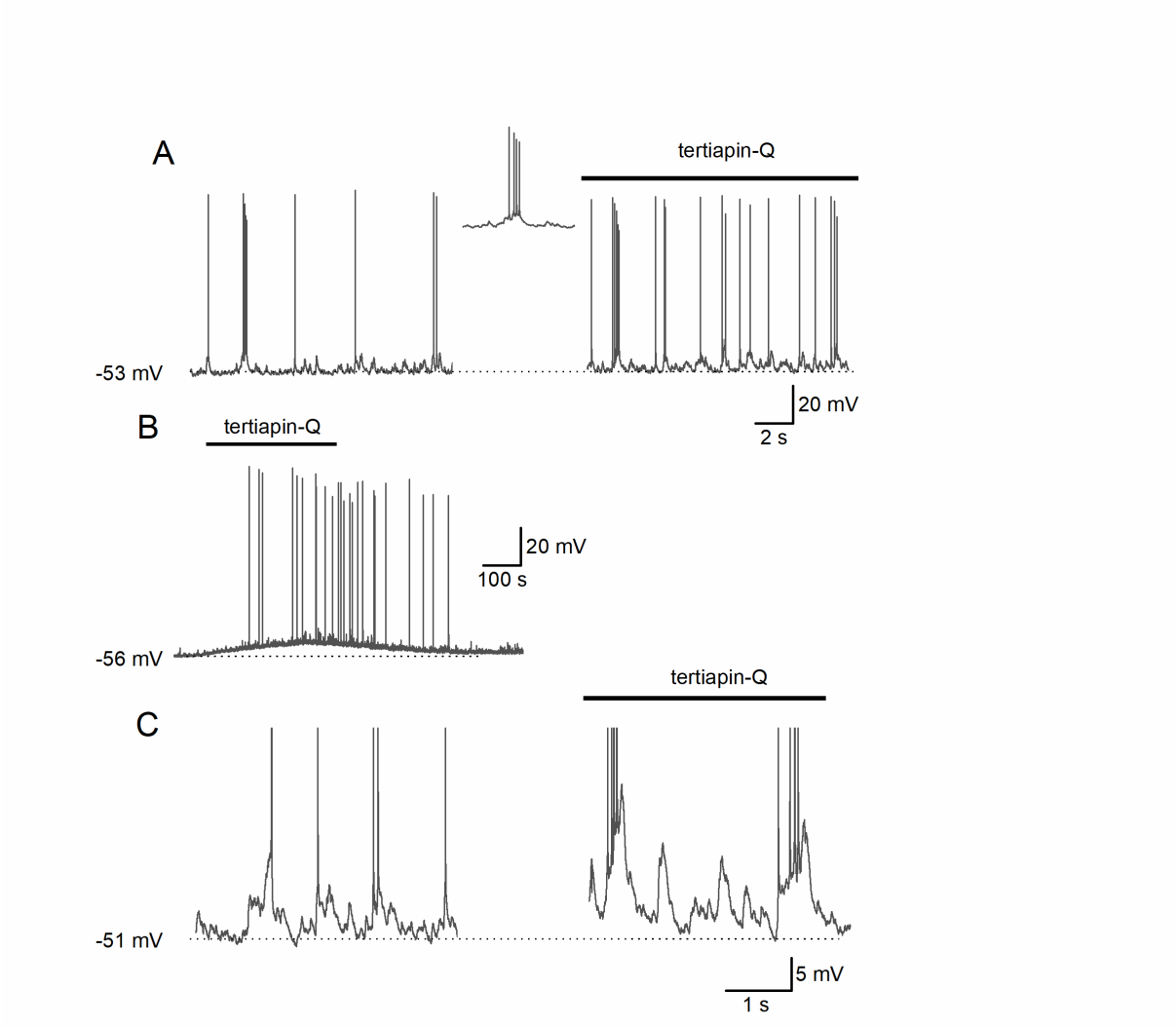
A
tertiapin-Q
-53 mV
20 mV
2 s
B
tertiapin-Q
20 mV
100 s
-56 mV
tertiapin-Q
C
-51 mV
5 mV
1 s

Figure 4

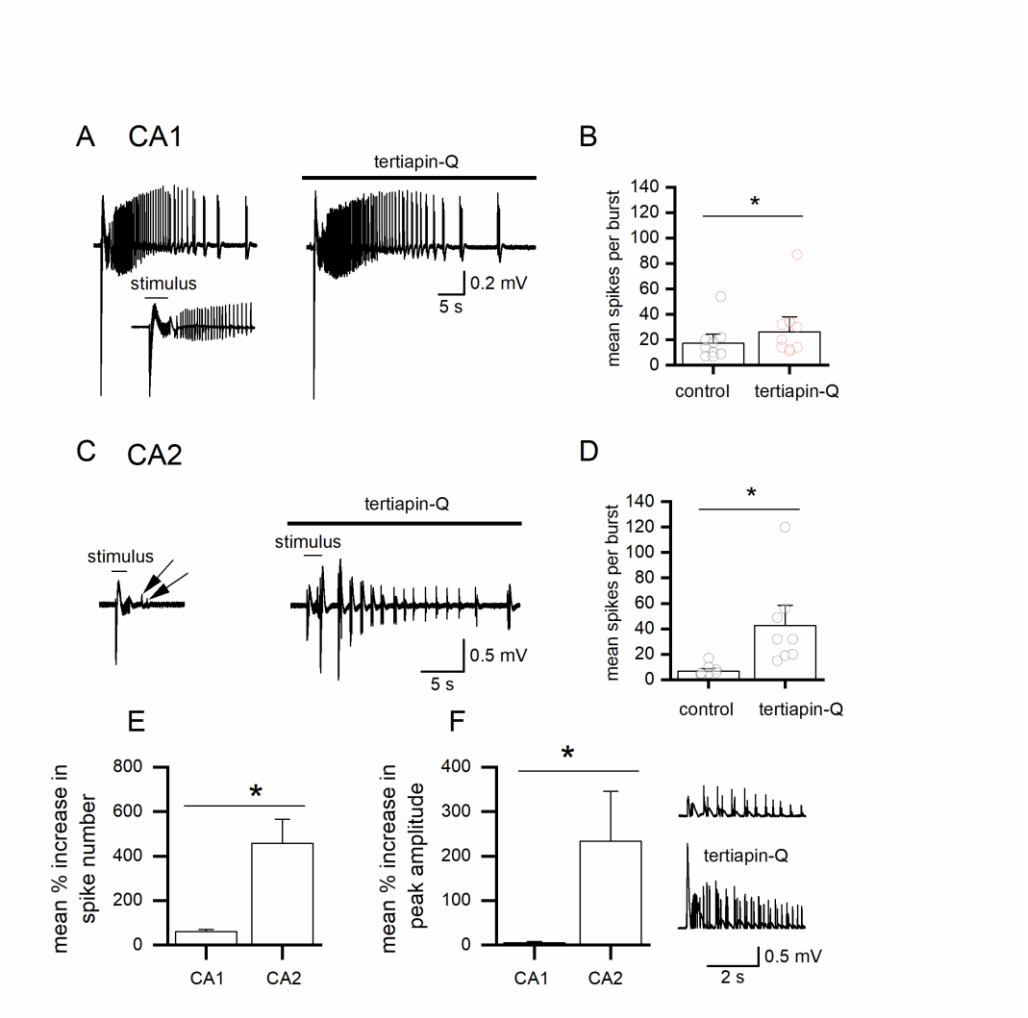
A
CA1
tertiapin-Q
stimulus
0.2 mV
5 s
B
mean spikes per burst
140
120
100
80
60
40
20
0
*
control
tertiapin-Q
C
CA2
stimulus
tertiapin-Q
stimulus
0.5 mV
5 s
D
mean spikes per burst
140
120
100
80
60
40
20
0
*
control
tertiapin-Q
E
mean % increase in spike number
800
600
400
200
0
*
CA1
CA2
F
mean % increase in peak amplitude
400
300
200
100
0
*
CA1
CA2
tertiapin-Q
0.5 mV
2 s

Figure 5

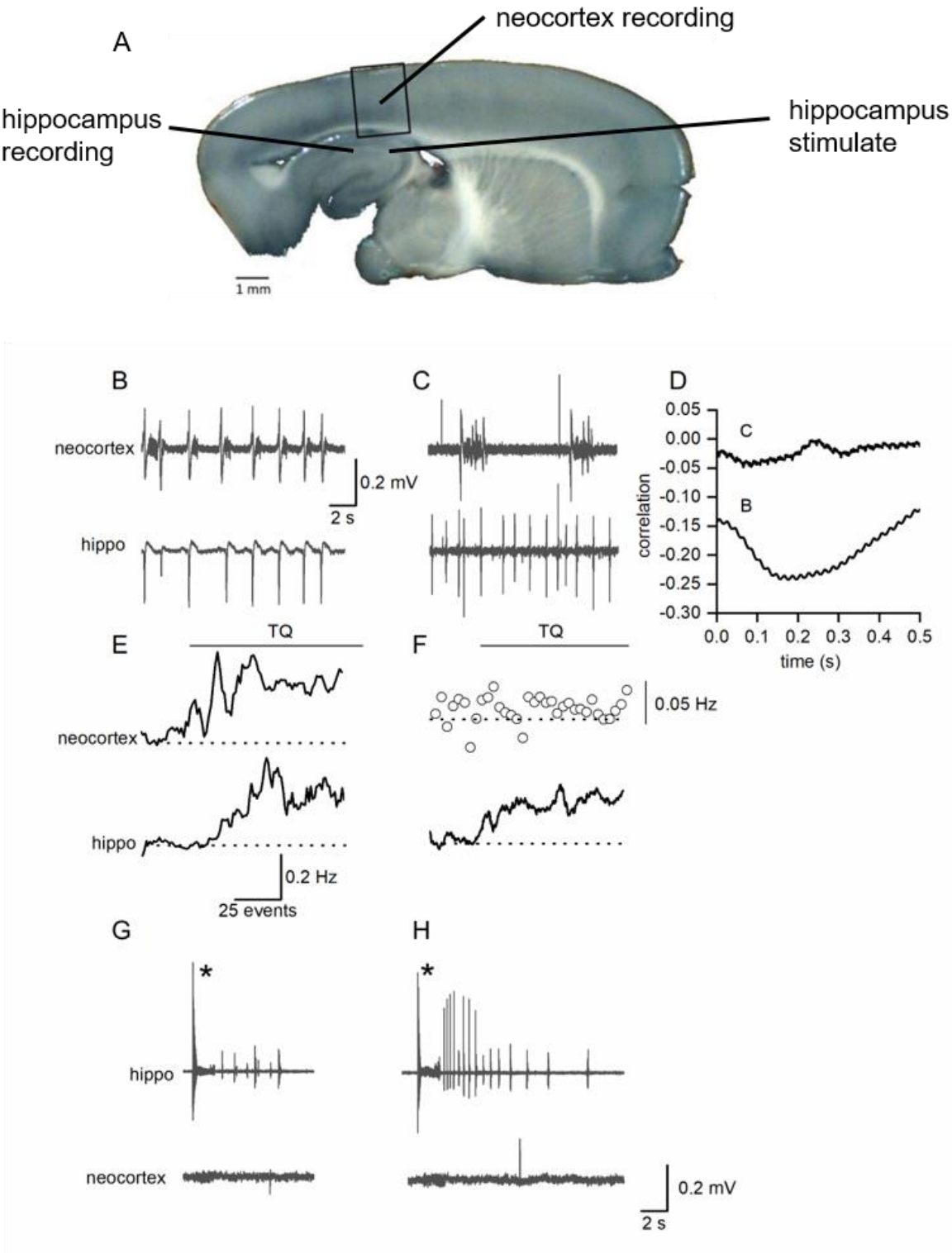
A
neocortex recording
hippocampus recording
hippocampus stimulate
1 mm
B
neocortex
0.2 mV
2 s
hippo
C
D
0.05
0.00
-0.05
-0.10
-0.15
-0.20
-0.25
-0.30
correlation
C
B
0.0 0.1 0.2 0.3 0.4 0.5
time (s)
E
TQ
neocortex
hippo
0.2 Hz
25 events
F
TQ
0.05 Hz
G
*
hippo
neocortex
H
*
0.2 mV
2 s

Figure 6.